

Synthesis of Chitosan Nanoparticles for Controlled Release of Amiodarone

N. I. BUYUK¹, P. P. ARAYICI, S. DERMAN, Z. MUSTAFAEVA AND S. YUCEL*

Department of Bioengineering, Yildiz Technical University, Davutpasa Street, Istanbul, 34220, ¹Department of Biotechnology, Yeditepe University, Istanbul, Turkey

Buyuk *et al.*: Amiodarone-loaded Chitosan Nanoparticles

This work is based on a natural polymer chitosan used in a nanoparticulate drug delivery system for the controlled release of amiodarone along with β -cyclodextrin. Amiodarone-loaded chitosan nanoparticles were prepared using the ionic gelation method aided by sonication. Amiodarone loading on chitosan nanoparticles was done under optimum conditions. For particle characterization; zeta-sizer, UV/Vis, Fourier-transform infrared spectroscopy, X-ray powder diffraction, differential scanning calorimeter and scanning electron microscope techniques were used. *In vitro* drug release studies of amiodarone-loaded chitosan nanoparticles were performed using the dialysis diffusion technique. Drug loading and release values were determined using UV/Vis spectroscopy. Amiodarone encapsulated in nanoparticles was completely released at the end of 14 days. About 38 % was released at the end of day 1, 44% released at the end of day 3, 50 % released at the end of day 5 followed slow release. Amiodarone-loaded chitosan nanoparticles could serve as a model for controlled delivery of many antiarrhythmic drugs.

Key words: Amiodarone, chitosan nanoparticles, cyclodextrin, drug release, ionic gelation method

The most commonly used natural polymer in drug release systems is chitosan (CS). CS is positively charged compared to other natural polymers and also biocompatible^[1]. It can leave the system without any side effects. If is nanostructured, it can be used in drug delivery systems. Advantages of nanoparticles (NP) are biocompatibility, biodegradability, low toxicity, control of the release of active agents, production without dangerous organic solvents, cross-linking due to free amine groups in the structure, easy ionic bonding with anion molecules since it is cationic, and mucoadhesive properties^[2-4]. The preparation method of CSNPs provides a higher affinity for negatively charged biological membranes and specific targeting *in vivo*. Thanks to its high affinity, it can be used in controlled drug delivery systems^[4].

Generally ionic gelation is used for producing CSNPs. The method was first developed in 1997 by Calvo^[5]. Physical cross-linkers are used because of the potential side effects of chemical cross-linkers in this method. The most extensively used crosslinker for this purpose is sodium tripolyphosphate (TPP), which is a polyanion and makes ionic interactions between CS chains^[5]. This method eliminates the need for organic solvents for the

production of NPs, the reaction can be accomplished in an aqueous solution and this avoids any damage to the activity of the drug since no high energy is needed during NP formation. Using ultrasonic waves to produce NP is one of the most efficient method used in recent times. In sonochemistry general frequency range varies between 20 kHz-1 MHz^[6], with this energy, the formation of aggregates in solution can be broken down, the particle size and also polydispersity index can be reduced^[7].

The use of ultrasonic method in nanotechnology has been widely accepted, but the number of studies on CS polymer are very few^[8]. Tang *et al.*^[8], Saha *et al.*^[9], Rafeeq *et al.*^[10] and Azelea *et al.*^[11] synthesized CSNPs by ionic gelation and then the samples were treated by sonication. After 2014; Gouda *et al.*^[12], Sugita *et al.*^[13], Xu *et al.*^[14] and Chouljenko *et al.*^[15] used only a sonicator device to produce CSNPs. These results

This is an open access article distributed under the terms of the Creative Commons Attribution-NonCommercial-ShareAlike 3.0 License, which allows others to remix, tweak, and build upon the work non-commercially, as long as the author is credited and the new creations are licensed under the identical terms

*Address for correspondence
E-mail: yuce.sevil@gmail.com

showed that sonication is helpful in many ways for production of CSNPs.

The production of polymeric NPs is particularly important in the treatment of diseases that require long-term therapy. Today, heart diseases are the most common cause of sudden death in the world. Many of the heart diseases are caused by rhythmic disorders. Antiarrhythmic drugs are widely used to treat rhythmic disorders^[16]. Amiodarone (AMD) is one of the most prescribed antiarrhythmic drug worldwide that is a class III antiarrhythmic drug^[17]. Although it has properties in class I, II and IV antiarrhythmic drugs, its main target is the blocking of the K channel. In addition, AMD is described as a multi-channel blocker because it can also block Na and Ca channels. Blocking the K channel prolongs atrial and ventricular repolarization time^[18]. It has a slowing effect on heart rate.

NPs, which have been widely prepared for controlled drug delivery has advantages such as, controlled release and ease of entry into the cell due to the fact that they are nano-sized. Natural polymers are desired drug release materials because of having the advantages of NPs.

This work is based on employing a natural polymer, CS due to its advantages, in drug delivery systems. In this study, an attempt was made to load AMD, one of the most commonly used antiarrhythmic drug, in biocompatible and biodegradable CSNPs for use in long-term treatment of heart diseases. Although antiarrhythmic drug-loaded CSNP studies are available in the literature^[19-21], the number of these studies is quite low due to the hydrophobicity and difficult encapsulation of the active substances. In these studies, organic solvents were generally used to dissolve such lipophilic drugs and this could cause carcinogenic or neurotoxic effects.

Since AMD is also hydrophobic, β -cyclodextrin (β -CD), which has been extensively used to increase the water solubility of hydrophobic molecules^[22-29], was added to enhance AMD solubility in water and allow it to be loaded into the CSNP. A Zeta-Sizer, UV/Vis spectrometry, Fourier-transform infrared (FTIR), X-ray diffraction (XRD), differential scanning calorimetry (DSC) and scanning electron microscopy (SEM) analytical techniques were used to characterize the NPs produced and controlled release of AMD from these NPs was determined in phosphate buffered saline (PBS).

MATERIALS AND METHODS

Chitosan (deacetylation degree- 75-85 %, medium molecular weight, product code: 448877), AMD hydrochloride (purity- 98 % purity, molecular weight- 681.77, product code- A8423) and sodium tripolyphosphate (molecular weight- 367.86, product code: 72061) were purchased from Sigma-Aldrich; β -cyclodextrin (molecular weight- 1134.98, product code- 1154569) was purchased from USP; was purchased from Sigma-Aldrich. All other chemicals used were of analytical grade.

AMD solubility studies:

AMD solubility studies were performed according the method of Higuchi *et al.*^[30]. Study was performed in two steps; in the first step, 20 mg β -CD was added to 10 ml pure water containing 1, 3, 5, 10 and 20 mg AMD, respectively. In the second step, AMD was added to 10 ml pure water containing 20, 25, 30, 35 and 40 mg β -CD, respectively. These were stirred on a magnetic stirrer at room temperature for 24 h. The solutions were filtered through 0.45 μ m syringe filters. The filtered solutions were analyzed by the UV spectrophotometer (Scinco, S-3100) at 242 nm^[31].

Preparation of the AMD-loaded CSNPs:

CSNPs were synthesized by the enhanced method of ionic gelation, which was developed by Calvo^[5] and then advanced using the ultrasonicator^[8,13,32]. The AMD- β -CD solution was added to the CS solution at a concentration of 4 mg/ml (w/v) and filtered through a 0.45 μ m syringe filter. The solution was stirred on a magnetic stirrer for 30 min to provide an interaction between CS and AMD. The TPP solution at a concentration of 2 mg/ml (w/v) was filtered through a 0.20 μ m syringe filter. Then, at room temperature, the ultrasonicator set for 5 min at 50 W with 30-10 pulse. The AMD-loaded NPs were synthesized by the mass ratio of 5:1 (CS:TPP). The synthesis conditions used in the study and given formulation codes (FC) are presented in the Table 1.

Particle size and surface charge determination:

A Zetasizer Nano ZS (Model ZEN0040, Malvern Instruments) was used for characterization. Particle size, zeta potential and polydispersity index (PDI) of blank and AMD-loaded NPs were determined by photon correlation spectroscopy. Blank and AMD-loaded CSNPs were prepared under the specified conditions. Dynamic light scattering (DLS) technique was used

TABLE 1: DIFFERENT SYNTHESIS CONDITIONS USED IN THE STUDY

FC	CS content (mg/ml)	TPP content (mg/ml)	β -CD content (mg/ml)	AMD content (mg/ml)
NP1	4	2	3.0	-
NP2	4	2	3.5	-
NP3	4	2	3.0	0.5
NP4	4	2	3.5	0.5

to calculate the average size of CSNPs. About 500 μ l of NP solution was loaded directly into the disposable cuvette of the zetasizer by placing it in the device^[33].

Morphology and FTIR analysis:

SEM (Zeiss, EVOLS10, Japan) was used to determine the morphological characteristics of NPs. For SEM analysis, one drop of freshly prepared NPs dropped onto the carbon band and the liquid part is evaporated at room temperature. The surface was coated with a gold-palladium complex under vacuum and then examined^[34]. Molecular characterization of blank and AMD-loaded CSNPs was performed on a IR-Prestige 21 FTIR spectrophotometer (Shimadzu, Japan). The device was set with resolution of 4 cm^{-1} and with frequency range of 650-4000 cm^{-1} .

XRD and DSC analyses:

The crystal structure of the synthesized NPs was measured by XRD. The XRD measurements were performed on an X'Pert PRO (PANalytical BV, Netherlands). X-ray diffraction patterns were recorded using Cu $K\alpha$ radiation, operated at 45 kV voltage and 40 mA current. The samples were recorded 0.025° step resolution, in the 2θ ranges from 10° to 60° for the AMD, blank and loaded NPs. DSC analysis was performed using DSC131 (Setaram, KEP Technologies, France) to learn NPs heat capacity changed by temperature. The phase behavior of CS, TPP, AMD, CD, blank and AMD loaded NPs was recorded. About 6 mg of samples for each were accurately weighed and sealed in an aluminum pan. Thermogram was recorded in a range of 50-350° with heating rate of 10°/min.

Evaluation of AMD-loaded NP reaction yield:

The reaction yield (RY) analysis of the AMD-loaded CSNPs was determined by gravimetric method. The CSNP suspension was centrifuged at +4°, 13 000 rpm for 30 min in a high-speed refrigerated centrifuge (Hitachi) with a 50-ml falcon tube. The supernatant was removed, the pellet was washed several times and the remaining pellet suspensions were lyophilized. using

an Alpha 1-2 LDplus lyophilizer. Fully dried NPs were weighed on a precision scale. The yield was calculated using the following Eqn., yield (%) = (weight of NPs)/(total weight of solids)×100.

Evaluation of encapsulation efficiency and loading capacity:

The encapsulation efficiency (EE) and loading capacity (LC) of the AMD-loaded CSNPs were measured using the supernatant collected after centrifugation of NPs. The absorbance value of the obtained supernatants was measured at 242 nm^[35]. AMD concentration was determined using the ϵ , molar absorption coefficient. The EE^[36] and LC^[37] were calculated using the Eqns. 2 and 3, EE (%) = (total amiodarone amount-amiodarone amount in supernatant)/(total amiodarone amount)×100; LC (%) = (total amiodarone amount-amiodarone amount in supernatant)/(weight of nanoparticles)×100.

In vitro release of AMD from CSNPs:

Determination of *in vitro* release was performed by placing the dried AMD-loaded CSNPs in a beaker containing 5 ml of PBS and 0.01 % sodium azide solution. The sample was sonicated and placed on a dialysis membrane (MWCO: 12.000 Da, D9777, Dialysis tubing cellulose membrane, Sigma). The dialysis membrane was placed in a beaker contains 50 ml of PBS. The temperature of the shaking water bath was adjusted to 37° and agitation was started at 100 rpm. Samples were withdrawn at specific time intervals and same volume of fresh PBS solution was replaced each time^[38]. The AMD concentration was determined on a UV/Vis spectrophotometer at 242 nm^[35].

RESULTS AND DISCUSSION

The phase solubility profiles for the complex formation between AMD and β -CD was shown in fig. 1. The

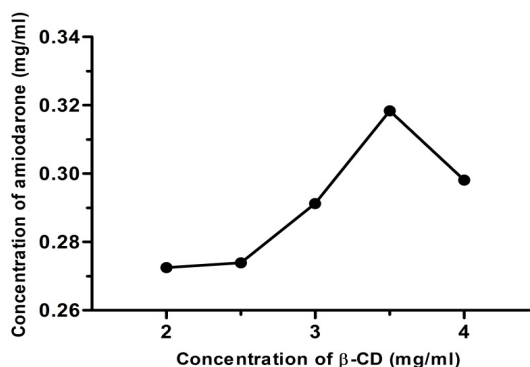


Fig. 1: Phase solubility of amiodarone with β -cyclodextrin
Phase solubility plot of amiodarone with β -cyclodextrin in distilled water at 25±0.5°

plot of the AMD β -CD solubility study indicated a characteristic Bs type phase solubility diagram^[39]. B type curves are seen in weakly soluble substances in water. The Bs type is found for materials with limited water solubility. It appears that AMD is dissolved in water in limited quantities because of the hydrophobic character^[16]. Only 30 % of the AMD was dissolved in water. It was decided to use solutions containing 30 and 35 mg of β -CD, which were the best conditions to dissolve. These two conditions had been used in all experiments in this study.

Particle size and zeta potential measurements were performed on a zetasizer. Dimensional analysis was performed and recorded. The results were presented in Table 2. The mean Z-avg sizes of blank NPs ranged from 172.5 \pm 8.19 to 228.3 \pm 9.73 nm while AMD-loaded NPs ranged from 296.8 \pm 4.14 to 372.8 \pm 11.53 nm. The intensity magnitudes of blank NPs varied from 216.4 \pm 15.70 to 363.7 \pm 40.21 nm while intensity magnitudes of AMD-loaded NPs varied between 377.4 \pm 31.44 to 484.5 \pm 45.33 nm. The size distribution

patterns were presented in fig. 2. It appeared that the size increased when AMD was loaded to NPs. Similarly Elzatahry *et al.*^[40] reported that blank NPs prepared with a mass ratio of 4:1 (CS:TPP), the blank NP diameter was 300 nm, which increased to 450 nm after metronidazole was loaded. Ye *et al.*^[26] synthesized blank NPs with a size of 238.5 to 391.2 nm and when these NPs were loaded with paclitaxel/dimethyl- β -CD, larger particles with diameters ranging from 440.2 to 521.4 nm were formed. In the present study also it was observed that the particle size increased with drug loading as reported in literature^[28,41-44].

Zeta potential values were found in the range of 26-28 mV in blank NPs and 29-30 mV in AMD-loaded NPs. There was no significant difference between the zeta potentials of blank and AMD-loaded CSNPs (Table 2). Since the zeta potential values are around 30 mV, the solution tends to be stable^[45].

The particle morphology characteristics of the AMD-loaded CSNPs were investigated using SEM. The SEM

TABLE 2: PHYSICO-CHEMICAL PROPERTIES OF BLANK AND AMIODARONE-LOADED CSNPs

FC	Z-avg (nm)	PDI	Intensity (nm)	Zeta Potential (mV)	RY (%)	EE (%)	LC (%)
NP1	172.5 \pm 8.2	0.39 \pm 0.048	216.4 \pm 15.7	+27.2	11.9	-	-
NP2	228.3 \pm 9.7	0.48 \pm 0.033	363.7 \pm 40.2	+26.0	11.8	-	-
NP3	296.8 \pm 4.1	0.41 \pm 0.023	377.4 \pm 31.4	+29.4	13.3	33.4	8.6
NP4	372.8 \pm 11.53	0.44 \pm 0.036	484.5 \pm 45.33	+29.7	14.2	35.6	8.8

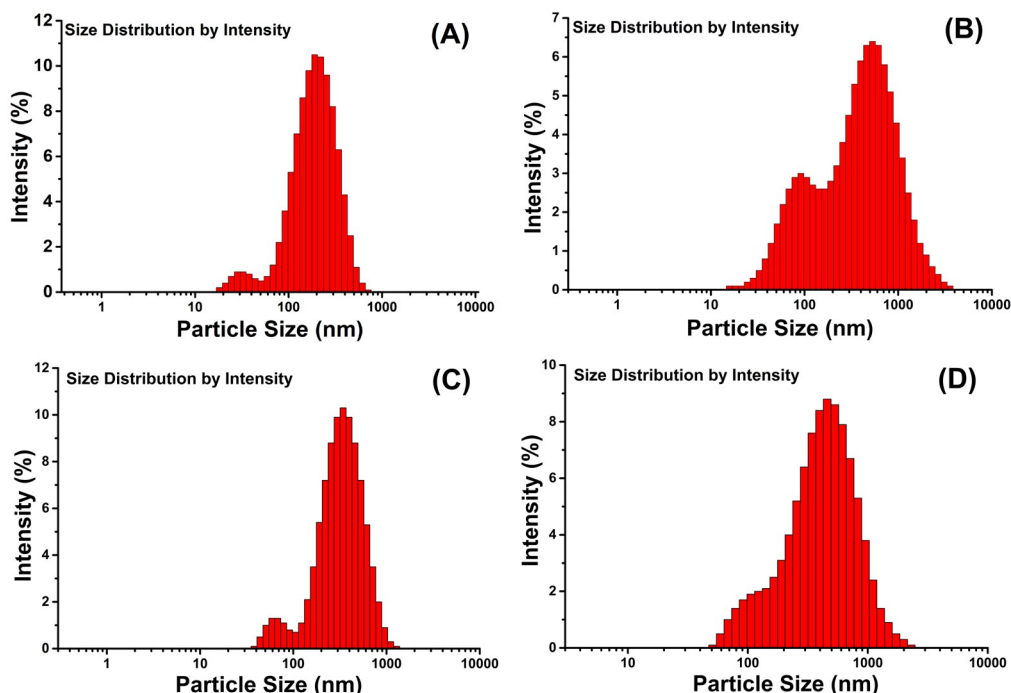


Fig. 2: CSNP particle size distribution
Particle size distribution of the Chitosan Nanoparticles (CANP) (A) NP1, (B) NP2, (C) NP3 and (D) NP4

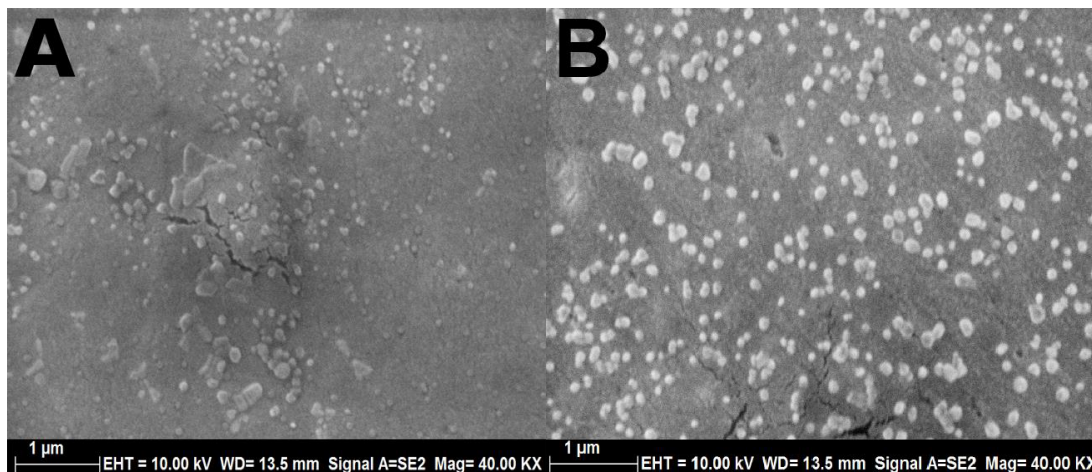


Fig. 3: Scanning electron pictomicrographs of AMD-loaded CSNPs
Scanning electron pictomicrographs of amidarone-loaded chitosan nanoparticles (AMD-loaded CSNP) (A) NP3, and (B) NP4, produced by sonication

image of AMD-loaded CSNPs was presented in the fig. 3. The results showed that AMD-loaded CSNPs were spherical in shape and had smooth surface. NP4 was bigger than the NP3 because of the increased loading content. The particle size results obtained using DLS and SEM image showed consistency.

The FTIR spectra of CS, AMD, β -CD, blank and AMD-loaded CSNPs are shown in fig. 4. Characteristic absorbance peaks of CS with medium molecular weight are 3396 and 3284 cm^{-1} , which are due to -NH and -OH stretching in CS. These peaks may also be due to hydrogen bonds for the molecule. The 2921 and 2850 cm^{-1} peaks are -CH symmetric and asymmetric stresses, respectively. These bands are characteristic for polysaccharides and are also found in other polysaccharides. As residues of N-acetyl groups of CS structure peaks are; 1640 cm^{-1} (C=O stretching), 1300 cm^{-1} (-CN stretching), 1545 cm^{-1} (-NH stretching), 1004 cm^{-1} (C-O stretching)^[46]. In the FTIR spectroscopy, the AMD molecule gives the characteristic peaks at 1620, 1557, 1170, 998 and 754 cm^{-1} . Stress vibrations of the group -C=O carbonyl appear at 1620 cm^{-1} ; the peaks at 1557 and 1446 cm^{-1} represent aromatic C=C stretching vibrations. Aliphatic CH stretching is presented at symmetrical and asymmetric stretching of 2931 and 2855 cm^{-1} , aromatic CH stretching at 2968 cm^{-1} , aliphatic CH₃ symmetric deformation at 1381 cm^{-1} , C=O stretching at 1620 cm^{-1} ^[35]. The peaks originating from -NH and -OH stretching in the CSNPs were found to expand to 3427, 3276 and 3157 cm^{-1} peaks, respectively, for AMD-loaded samples. This situation is thought to be due to the expansion of H bonds^[47]. It observed that 1640 cm^{-1} peak in the CS is protected in NPs however 1545 cm^{-1} absorbance peak shifted to 1552 cm^{-1} . This

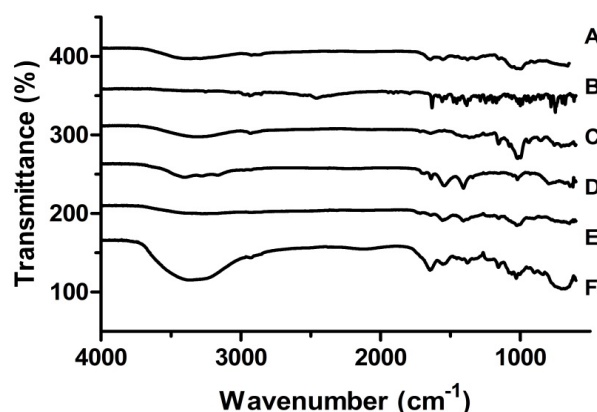


Fig. 4: FTIR spectra
(A) Chitosan, (B) amidarone, (C) β -CD, (D) blank chitosan nanoparticles, (E) amidarone-loaded chitosan nanoparticle NP3, (F) amidarone-loaded chitosan nanoparticle NP4

is thought to be due to the cross-linking of -NH bonds with TPP. A new peak formation originating from P=O bond was observed at 1209 cm^{-1} ^[48]. This is due to the formation of bonds between the amino groups present in the CS and the phosphate groups present in TPP. The characteristic peaks of AMD disappear after NP production. This situation proves that the drug is effectively encapsulated^[49].

The physical state of AMD, blank and loaded NPs were subjected to XRD analysis. The diffraction spectrums of samples were presented in fig. 5. While AMD shows significant peaks at 21.46°, 23.47°, 27.17° due to its crystal structure, it was seen that the intensity peaks in blank and loaded nanoparticles is diminished. This proved that AMD was loaded into chitosan nanoparticles quite successfully. At the same time, AMD in nanoparticles lost its crystallinity, which is a less soluble form to its amorphous form. Studies reported in literature support this finding^[50]. The

magnitude of the peaks obtained as a result of XRD was associated with the crystalline form of the material. According to XRD results obtained from nanoparticles, these peaks seem to be quite low, which was thought to be caused by the loss of the crystal structure of chitosan as a result of cross-linking with TPP^[22].

The phase transition curves of CS, TPP, AMD, β -CD, blank and empty NPs are presented in fig. 6. In CS thermogram two peaks exhibited: an endothermic peak at 120.27° due to loss of water and exothermic peak at 310.72° due to decomposition of amine groups^[51]. AMD showed a single sharp endothermic peak at 172.77° according to the melting temperature of the drug. Thermogram of CD showed two endothermic peaks at 140.67° and 279.06°. In addition, thermogram of TPP showed two endothermic peaks at 121.05° and 206.98° corresponding to melting point of crystalline region. Blank and loaded NPs had an endothermic peak at 107.91° and 97.59° and also another endotherm peak at 275.63 and 277.6°, respectively. In NPs characteristics

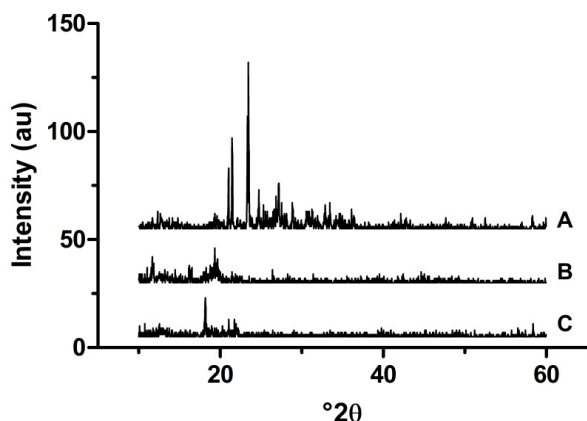


Fig. 5: XRD spectra
(A) Amiodarone, (B) blank chitosan nanoparticles, (C) amiodarone-loaded chitosan nanoparticles

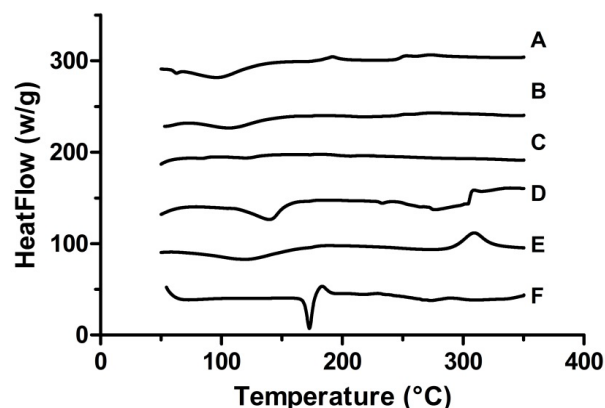


Fig. 6: DSC spectra
(A) Amiodarone-loaded chitosan nanoparticles, (B) blank chitosan nanoparticles, (C) TPP, (D) β -CD, (E) chitosan, (F) amiodarone

peaks of CS and β -CD were joint and could be observed. There were no endothermic peak for AMD in loaded NPs, which showed that AMD had been incorporated with β -CD^[50]. Similar results were obtained in the literature^[52].

The RY of blank and AMD-loaded CSNPs varied between 11-15 % (Table 2). AMD-loaded NPs showed low RY values. No significant difference was observed in RYs between NPs loaded with different amounts of CD. RY was higher in NPs loaded with active substance than blank NPs, which was thought to be due to the fact that CD, which capsulated AMD, forms a stronger bond with CS to produce NPs. In the study of Trapani *et al.* loading materials with low water solubility into CSNP, the RY remained in the range of 8-13 % which was an acceptable range for hydrophobic materials^[25].

The EE of AMD-loaded CSNPs varied between 33 and 36 %. The EE results of this study showed similar trends to what was reported in the literature^[26]. The LC of AMD-loaded CSNPs varied between 8-9 % (Table 2). Although the results obtained in this study are similar to the previous studies^[25], the LC in this study is slightly more effective^[42]. It was found that increasing the amount of CD in NPs, which is used to increase the solubility of AMD, also increased the EE and LC of CSNPs, but this increase is not significant. Although it is convenient for such molecules to increase the amount of CD used for loading hydrophobic materials to chitosan, it is seen that EE and LC are lower compared to other studies performed for loading hydrophilic materials^[31,36,44].

Release studies on AMD-loaded CSNPs were carried out in triplicate. Two different doses of drug-loaded NP were used to study release. The study was continued for 20 d. Concentration calculations were made with UV measurements taken at specific time intervals, these values were converted to mg, and fig. 7 was drawn to determine to find the drug release percentage with time. It appears that the NPs which contained 5 mg AMD and 30 mg β -CD release all of the AMD it's include at the end of the release study. It took 14 d for the CSNPs to release 100 % of the drug. About 32 % of the active substance was released within the first 5 h, followed by a slow release. After 14 d, the work was continued without interruption and was shown to be stable. It can be seen that the release of all of AMD in NP4 could not be achieved. It was observed that the CSNP, which released 22 % of AMD loaded in the first 4 h, slowed down the process to released up to 40 % of AMD. This difference between the two NPs produced is thought

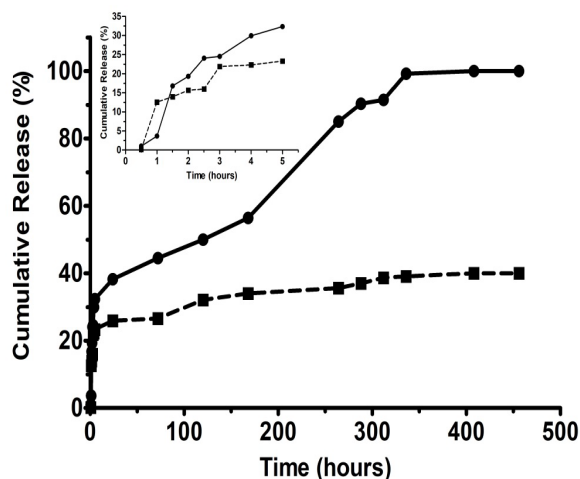


Fig. 7: *In vitro* drug release from amiodarone-loaded CSNPs
In vitro drug release study of amiodarone-loaded chitosan nanoparticles NP3 (—●—) and NP4 (---■---)

to be caused by the change in the amount of CD it contains. The CD in the solution provided a tighter binding to the NP, resulting in slowing of release. Recent studies showed that adding CD improved the LC despite slowing down drug release^[53,54].

In summary, AMD was loaded to CSNPs successfully. Solubility studies were performed with β -CD due to the hydrophobic nature of AMD. AMD: β -CD (1:7) mass ratio was the optimal combination. In the Zetasizer results, it was observed that the NPs were of the optimal size and had monodispersed particle distribution. SEM images showed spherical structure. The fact that the encapsulation of AMD was successful was obtained from the FTIR, DSC and XRD results. DSC and XRD analysis indicated that physical state of AMD transformed into more amorphous state. AMD-loaded NPs had a RY of 11-15 %, an EE of 33-36 % and a LC of 8-9 % in this study. In *in vitro* release studies, all of the AMD was released after 14 d, 38 % at the end of day 1, 44 % at the end of day 3, and 50 % at the end of day 5. It is thought that NPs produced in this study could be used for long-term treatment with AMD and also could serve as a model for controlled delivery of many antiarrhythmic drugs.

REFERENCES

1. Yao KD, Yin YJ, Xu MX, Wang YF. Investigation of pH-sensitive drug delivery system of chitosan/gelatin hybrid polymer netw. *Polym Int* 1995;38:77-82.
2. Peniche C, Argüelles-Monal W, Goycoolea FM. Chitin and Chitosan: Major Sources, Properties and Applications. In: van den Broek LAM, Boeriu CG, Stevens CV, editors. *Monomers, polymers and composites from renewable resources*. Amsterdam: Elsevier; 2008. p. 517-42.
3. Gan Q, Wang T. Chitosan nanoparticle as protein delivery carrier-Systematic examination of fabrication conditions for efficient loading and release. *Colloids Surfaces B Biointerfaces* 2007;59(1):24-34.
4. Perera UMSP, Rajapakse N. Seafood Processing By-Products. In: Se-Kwon K, editors. *Chitosan Nanoparticles: Preparation, Characterization, and Applications*. New York: Springer; 2013. P. 371-87.
5. Calvo P, Lopez CR, Vila-Jato JL, Alonso MJ. Novel Hydrophilic Chitosan – Polyethylene Oxide Nanoparticles as Protein Carriers. *J Appl Polym Sci* 1997;63:125-32.
6. Schroeder A, Kost J, Barenholz Y. Ultrasound, Liposomes, and Drug Delivery: Principles for using Ultrasound to Control the release of Drugs from Liposomes. *Chem Phys Lipids* 2009;162:1-16.
7. Tsai M, Bai S, Chen R. Cavitation effects versus stretch effects resulted in different size and polydispersity of ionotropic gelation chitosan–sodium tripolyphosphate nanoparticle. *Carbohydr Polym* 2008;71:448-57.
8. Tang ESKSK, Huang M, Lim LYY. Ultrasonication of chitosan and chitosan nanoparticles. *Int J Pharm* 2003;265(1-2):103-14.
9. Saha P, Goyal AK, Rath G. Formulation and evaluation of chitosan-based ampicillin trihydrate nanoparticles. *Trop J Pharm Res* 2010;9(5):483-8.
10. Rafeeq MP, Junise V, Saraswathi R, Krishnan P. Development and characterization of chitosan nanoparticles loaded with isoniazid for the treatment of Tuberculosis. *Res J Pharm Biol Chem Sci* 2010;1(4):383-90.
11. Azalea DR, Mohamed M, Joji S, Sankar CBM. Design and Evaluation of Chitosan Nanoparticles as Novel Drug Carriers for the Delivery of Donepezil. *Iran J Pharm Sci* 2012;8(3):155-64.
12. Gouda M, Elayaan U, Youssef MM. Synthesis and Biological Activity of Drug Delivery System Based on Chitosan Nanocapsules. *Synth Biol Act Drug Deliv Syst Based Chitosan Nanocapsules Adv Nanoparticles* 2014;3(3):148-58.
13. Sugita P, Ambarsari L, Lidiniyah. Optimization of ketoprofen-loaded chitosan nanoparticle ultrasonic process. *Procedia Chem* 2015;16:673-80.
14. Xu F, Zhao T, Wang S, Wang H, Cui X. Preparation of magnetic and pH-responsive chitosan microcapsules via sonochemical method. *J Microencapsul* 2016;33(2):191-8.
15. Chouljenko A, Chotiko A, Solval MJ, Solval K, Sathivel S. Chitosan Nanoparticle Penetration into Shrimp Muscle and its Effects on the Microbial Quality. *Food Bioprocess Technol* 2017;10(1):186-98.
16. Gill J, Heel RC, Fitton A. Amiodarone. An overview of its pharmacological properties, and review of its therapeutic use in cardiac arrhythmias. *Drugs* 1992;43(1):69-110.
17. Marcus FI, Fontaine GH, Frank R, Grosogoeat Y. Amiodarone: the experience of the past decade. *Am Heart J* 1981;101:480-93.
18. Vassallo P, Trohman RG. Prescribing Amiodarone. *JAMA* 2007;298(11):1312-22.
19. Patil R, Pande V, Sonawane R. Nano and microparticulate chitosan based system for formulation of carvedilol rapid melt tablet. *Adv Pharm Bull* 2015;5(2):169-79.
20. Khan M saleh, Gowda DV, Shivakumar HG. Porous nanoparticles of metoprolol tartrate produced by spray-drying: Development, characterization and *in vitro* evaluation. *Acta Pharm* 2012;62(3):383-94.
21. Duangjit S, Kraisit P, Luangtana-Anan M. An investigation of propranolol-loaded chitosan nanoparticles for transmucosal delivery: Physical characterization. *Thai J Pharm Sci* 2016;40:25-8.

22. Jingou J, Shilei H, Weiqi L, Danjun W, Tengfei W, Yi X. Preparation, characterization of hydrophilic and hydrophobic drug in combine loaded chitosan/cyclodextrin nanoparticles and *in vitro* release study. *Colloids Surfaces B Biointerfaces* 2011;83(1):103-7.
23. Ji J, Hao S, Liu W. Preparation and evaluation of O-carboxymethyl chitosan/cyclodextrin nanoparticles as hydrophobic drug delivery carriers. *Polym Bull* 2011;67(7):1201-13.
24. Vyas A, Saraf S, Saraf S. Encapsulation of cyclodextrin complexed simvastatin in chitosan nanocarriers: A novel technique for oral delivery. *J Incl Phenom Macrocycl Chem* 2010;66(3):251-9.
25. Trapani A, Sitterberg J, Bakowsky U, Kissel T. The potential of glycol chitosan nanoparticles as carrier for low water soluble drugs. *Int J Pharm* 2009;375(1-2):97-106.
26. Ye YJ, Wang Y, Lou KY, Chen YZ, Chen R, Gao F. The preparation, characterization, and pharmacokinetic studies of chitosan nanoparticles loaded with paclitaxel/dimethyl- β -cyclodextrin inclusion complexes. *Int J Nanomedicine* 2015;10:4309-19.
27. Jingou J, Jingfen Z, Shilei H, Danjun WU, Li L, Yi X. Preparation, Characterization of Hydrophobic Drug in Combine Loaded Chitosan / Cyclodextrin / Trisodium Citrate Nanoparticles and *in vitro* Release Study. *Chem Res Chin Univ* 2012;28(1):166-70.
28. Gadade DD, Pekamwar S. Cyclodextrin Based Nanoparticles for Drug Delivery and Theranostics. *Adv Pharm Bull* 2019;19:28.
29. Menezes PDP, Andrade TA, Frank LA, de Souza EPBSS, Trindade GDGG, Trindade IAS, *et al.* Advances of nanosystems containing cyclodextrins and their applications in pharmaceuticals. *Int J Pharm* 2019;559:312-28.
30. Higuchi T, Connors KA. Phase-solubility techniques. *Adv Anal Chem Instrum* 1965;4:117-212.
31. Lu L, Shao X, Jiao Y, Zhou C. Synthesis of chitosan- graft β -cyclodextrin for improving the loading and release of doxorubicin in the nanoparticles. *J Appl Polym Sci* 2014;131(21):1-7.
32. Li J, Huang Q. Rheological properties of chitosan-tripolyphosphate complexes: From suspensions to microgels. *Carbohydr Polym* 2012;87(2):1670-7.
33. Mertz MW. Characterization of Novel Chitosan/Polyelectrolyte Nanoparticles, *Biomedical Engineering Undergraduate Honors Theses [dissertation]*. Fayetteville, AR: University of Arkansas; 2015.
34. Arasoglu T, Derman S, Mansuroglu B, Yelkenci G, Kocyigit B. Synthesis, Characterization and Antibacterial Activity of Juglone Encapsulated PLGA Nanoparticles. *J Appl Microbiol* 2017;123:1407-19.
35. Bonati M, Gaspari F, D'Aranno V, Benfenati E, Neyroz P, Galletti F. Physicochemical and analytical characteristics of amiodarone. *J Pharm Sci* 1984;73(6):829-31.
36. Dounighi M, Eskandari R, Zolfagharian H, Mohammad M. Preparation and *in vitro* characterization of chitosan nanoparticles containing Mesobuthus eupeus scorpion venom as an antigen delivery system. *J Venom Anim Toxins Incl Trop Dis* 2012;18(1):44-52.
37. Liu Y, Sun Y, Li YL, Xu SC, Xu YX. Characteration of Protein Loaded Chitosan Nanoparticles at Different pH Values. *Adv Mater Res* 2011;5:284-286, 950-3.
38. Arasoglu T, Derman S, Mansuroglu B. Comparative evaluation of antibacterial activity of caffeic acid phenethyl ester and PLGA nanoparticle formulation by different methods. *Nanotechnology* 2015;27:1-12.
39. Loftsson T, Brewster ME, Ru RR. Remington: The Science and Practice of Pharmacy Sample Chapter. In: Troy D, Beringe P, editors. *Complex Formation*. Philadelphia, Pennsylvania, United States: Lippincott Williams & Wilkins; 2006. p. 681-92.
40. Elzatahry AA, Eldin MSM. Preparation and characterization of metronidazole-loaded chitosan nanoparticles for drug delivery application. *Polym Adv Technol* 2008;19(12):1787-91.
41. Hou X, Zhang W, He M, Lu Y, Lou K, Gao F. Preparation and characterization of β -cyclodextrin grafted N-maleoyl chitosan nanoparticles for drug delivery. *Asian J Pharm Sci* 2017;12:558-68.
42. Tang P, Sun Q, Zhao L, Pu H, Yang H, Zhang S. Mesalazine/hydroxypropyl- β -cyclodextrin/chitosan nanoparticles with sustained release and enhanced anti-inflammation activity. *Carbohydr Polym* 2018;198:418-25.
43. Matshetshe KI, Parani S, Manki SM, Oluwafemi OS. Preparation, characterization and *in vitro* release study of β -cyclodextrin/ chitosan nanoparticles loaded Cinnamomum zeylanicum essential oil. *Int J Biol Macromol* 2018;118:676-82.
44. He M, Zhong C, Hu H, Jin Y, Chen Y, Lou K. Cyclodextrin/chitosan nanoparticles for oral ovalbumin delivery: Preparation, characterization and intestinal mucosal immunity in mice. *Asian J Pharm Sci* 2019;14(2):193-203.
45. Kumar A, Dixit CK. Methods for characterization of nanoparticles. *Adv Nanomedicine Deliv Ther Nucleic Acids* 2017;43:58.
46. Queiroz MF, Melo KRT, Sabry DA, Rocha HAO. Does the Use of Chitosan Contribute to Oxalate Kidney Stone Formation? *Mar Drugs* 2014;13(1):141-58.
47. Xu Y, Du Y. Effect of molecular structure of chitosan on protein delivery properties of chitosan nanoparticles. *Int J Pharm* 2003;250(1):215-26.
48. Qi L, Xu Z. Lead sorption from aqueous solutions on chitosan nanoparticles. *Colloids Surfaces A Physicochem Eng Asp* 2004;251(1):183-90.
49. Malhotra M, Lane C, Tomaro-Duchesneau C, Saha S, Prakash S. A novel method for synthesizing PEGylated chitosan nanoparticles: strategy, preparation, and *in vitro* analysis. *Int J Nanomedicine* 2011;6:485-94.
50. Kandav G, Bhatt DC, Jindal DK. Formulation and evaluation of allopurinol loaded chitosan nanoparticles. *Int J Appl Pharm* 2019;11(3):49-52.
51. Ferrero F, Periolatto M. Antimicrobial finish of textiles by chitosan UV-curing. *J Nanosci Nanotechnol* 2012;12(6):4803-10.
52. Campos EVR, Proença PLF, Oliveira JL, Melville CC, Della Vecchia JF, de Andrade DJ. Chitosan nanoparticles functionalized with β -cyclodextrin: a promising carrier for botanical pesticides. *Sci Rep* 2018;8(1):2067.
53. Singla AK, Sharma ML, Dhawan S. Nifedipine loaded chitosan microspheres: characterization of internal structure. *Biotech Histochem* 2001;76:165-71.
54. Rao VM, Haslam JL, Stella VJ. Controlled and complete release of a model poorly water-soluble drug, prednisolone, from hydroxypropyl methylcellulose matrix tablets using (SBE) γ -m- β -cyclodextrin as a solubilizing agent. *J Pharm Sci* 2001;90(7):807-16.